JVSTB Journal of Vacuum Science & Technology B

# Dielectrophoretic manipulation of individual nickel nanowires for electrical transport measurements

Marcos V. Puydinger dos Santos, Lucas P. B. Lima, Rafael A. Mayer, Fanny Béron, Kleber R. Pirota, and Jose A. Diniz

Citation: Journal of Vacuum Science & Technology B **33**, 031804 (2015); doi: 10.1116/1.4918732
View online: http://dx.doi.org/10.1116/1.4918732
View Table of Contents: http://scitation.aip.org/content/avs/journal/jvstb/33/3?ver=pdfcov
Published by the AVS: Science & Technology of Materials, Interfaces, and Processing



# Dielectrophoretic manipulation of individual nickel nanowires for electrical transport measurements

Marcos V. Puydinger dos Santos[a)]
*Institute of Physics "Gleb Wataghin," University of Campinas, 13083-859 Campinas, São Paulo, Brazil and School of Electrical and Computer Engineering, University of Campinas, 13083-970 Campinas, São Paulo, Brazil*

Lucas P. B. Lima
*School of Electrical and Computer Engineering and Center for Semiconductor Components, University of Campinas, 13083-970 Campinas, São Paulo, Brazil and Chemistry Department, Katholieke Universiteit Leuven, 3000 Leuven, Belgium*

Rafael A. Mayer, Fanny Béron, and Kleber R. Pirota
*Institute of Physics "Gleb Wataghin," University of Campinas, 13083-859 Campinas, São Paulo, Brazil*

Jose A. Diniz
*School of Electrical and Computer Engineering and Center for Semiconductor Components, University of Campinas, 13083-970 Campinas, São Paulo, Brazil*

(Received 2 December 2014; accepted 10 April 2015; published 22 April 2015)

Nanowires (NW) have received much attention due to their high aspect ratio, shape anisotropy, relatively large surface area and particular electron transport properties. In addition, since NW present low current levels and high sensitivity, they can be used as sensor devices for several applications. One of the major challenges when dealing with transport measurements in NW is to trap them between electrodes, which allow electrical characterization and therefore fabrication of nanowire-based devices. Electrically neutral NW can be deposited by dielectrophoresis (DEP) method, which requires the application of an alternating electric field between electrodes. In this work, properly dispersed Ni nanowires (NiNW) (length $= 4 \pm 1\ \mu$m, diameter $= 35 \pm 5$ nm) were deposited on top of Pt electrodes using the DEP method. The effects of electrodes geometry and electric field frequency on DEP efficiency were evaluated. For optimized DEP parameters, the process efficiency is up to 85%. The deposited NiNW exhibit a Schottky-like current versus voltage behavior due to the high contact resistance between NiNW and electrode. Its reduction down to two orders of magnitude, reaching value less than the NiNW resistance ($\sim$6 k$\Omega$), was achieved by depositing a 10 nm-thick Pt layer over the NW extremities. Therefore, this method presents a selection of adequate electrical DEP parameters and electrode geometry, making it a suitable process of NW deposition and electrical characterization. This can be used for investigation of electrical transport properties of individual NW and fabrication of NW-based devices, like sensors and field effect transistors. © *2015 American Vacuum Society*. [http://dx.doi.org/10.1116/1.4918732]

## I. INTRODUCTION

Nanowires (NW) are appropriate elements for electronic devices that require ultralow power consumption, given the low current levels and high sensitivity they usually exhibit.[1–5] One challenge to fabricate and study electrical transport properties of NW-based devices, such as semiconductor- and carbon-based transistors, is the appropriate manipulation of the NW toward electrodes.[6,7] So far, devices have been fabricated by several techniques, including electron beam lithography, focused ion beam (FIB) and atomic force microscopy manipulation, although with relatively low throughput.[5]

Alternatively, metallic NW suspended in a dielectric liquid medium can be directly manipulated through electric fields.[1,5,8–12] When a neutral NW is placed inside a nonuniform electric field region, the electric charges are redistributed within the NW and in the liquid portion of the liquid–solid interface, building up a dipole moment.[13] Since the Coulomb forces on either sides of the dipole moment can be different, a net force is exerted on the NW, which is known as the dielectrophoretic force.[6,8–13] This force direction depends on the relative polarizabilities of the NW and of the diluting medium, inducing the former to move toward or against the region of higher electric field intensity.[6,8–13] Such motion is called dielectrophoresis (DEP).[6–14]

Unlike the other techniques aforementioned, large electrodes array can be properly defined by lithography such that DEP can take place concomitantly in a large number of electrodes, leading to high throughput. Moreover, since DEP directly depends on the dielectric properties of the particles and diluting medium, it allows high selectivity and sensitivity analysis.[13,15] DEP manipulation can be also controlled by varying the frequency and magnitude of the applied electric field.[13]

In this work, properly isolated Ni nanowires (NiNW), with length of around 4 $\mu$m and 35 nm of diameter, obtained by electrodeposition into pores of anodized alumina membrane, were dispersed in a dimethylformalmide (DMF) solution and dielectrophoretically manipulated to make electrical

a)Electronic mail: puyding@ifi.unicamp.br

contact between electrodes. Electrodes geometry and DEP electrical parameters were varied to evaluate the NiNW deposition efficiency by this technique. In addition, electrical characterizations of the NW and of the contact resistance between the NW and electrode were performed by current versus voltage curves. Significant reduction of contact resistance was achieved by ion-beam assisted deposition of Pt cap layers on the NW extremities.

## II. DIELECTROPHORESIS

DEP uses nonuniform AC electric fields to selectively move neutral metallic NW dispersed in a dielectric diluting medium (i.e., DMF) [Fig. 1(a)]. It relies on the polarizability differences between the NW and the DMF. The electrodes shape yield to a nonuniform electric field, $E$, which is proportional to the applied voltage [Fig. 1(b)]. It creates a net force, $F_{\mathrm{DEP}}$, on the NW that exceeds the viscous force between the NW and the fluid, inducing a preferential NW movement toward the electrodes gap [Fig. 1(c)]. This force can be expressed by[5,11,16]

$$F_{\mathrm{DEP}} = \frac{1}{8}\pi\varphi^2 L\varepsilon_{\mathrm{DMF}}\mathrm{Re}\{K\}\nabla|E|^2, \tag{1}$$

where $\mathrm{Re}\{K\}$ is the real-term of the complex polarization factor, expressed as function of electrical permittivities of NiNW and DMF (respectively, $\varepsilon_{\mathrm{NiNW}}$ and $\varepsilon_{\mathrm{DMF}} = 36.7\varepsilon_0$, where $\varepsilon_0$ is the electrical permittivity of vacuum)[5]

$$\mathbf{K} = \frac{\left[\boldsymbol{\varepsilon}^*_{\mathrm{NiNW}} - \boldsymbol{\varepsilon}^*_{\mathrm{DMF}}\right]}{\boldsymbol{\varepsilon}^*_{\mathrm{DMF}}}. \tag{2}$$

The imaginary component of the complex permittivity, $\varepsilon^*$, depends of the conductivity, $\sigma$, and the applied field angular frequency, $\omega$,[5]

$$\boldsymbol{\varepsilon}^* = \boldsymbol{\varepsilon} - \boldsymbol{j}\frac{\boldsymbol{\sigma}}{\boldsymbol{\omega}}. \tag{3}$$

Thus, the real-term frequency dependent factor of the dielectrophoretic force is given by[5]

$$\boldsymbol{Re}\{\mathbf{K}\} = \frac{\boldsymbol{\omega}^2(\boldsymbol{\varepsilon}_{\mathrm{DMF}}\boldsymbol{\varepsilon}_{\mathrm{NiNW}}) + \left(\boldsymbol{\sigma}_{\mathrm{DMF}}\boldsymbol{\sigma}_{\mathrm{NiNW}} - \boldsymbol{\sigma}^2_{\mathrm{DMF}}\right)}{\boldsymbol{\varepsilon}^2_{\mathrm{DMF}}\boldsymbol{\omega}^2 + \boldsymbol{\sigma}^2_{\mathrm{DMF}}}. \tag{4}$$

Inserting the appropriate NW and diluting liquid electrical conductivities (respectively, $\sigma_{\mathrm{NiNW}} = 1.4 \times 10^7 \Omega^{-1}\mathrm{m}^{-1}$ and $\sigma_{\mathrm{DMF}} = 2.5 \times 10^{-4}\Omega^{-1}\mathrm{m}^{-1}$) in Eq. (4), one may calculate the frequency-dependence of $F_{\mathrm{DEP}}$, where a reduction of DEP force for frequencies higher than 100 kHz is observed (Fig. 2). At 500 kHz and 1 MHz, the force decreases by one and two orders of magnitude, respectively. However, this model does not consider fluid dynamics effects, such as electro-osmosis.[7] For the electrostatic parameters of NiNW and DMF, this effect can reduce the force for frequencies below 10 kHz,[6] as will be presented in Sec. IV. Other effects also act on the NW, such as viscous and frictional forces, fluid flow, and NW–surface interactions.[5,17] The DEP force therefore needs to be greater than calculated in order to effectively perform deposition.

Furthermore, Eq. (1) exhibits a quadratic dependence of DEP force with the applied voltage, which increases the amount of deposited NW in the gap region.[5] In this work, we fixed the peak-to-peak voltage ($V_{\mathrm{PP}}$) to 3 V, since it a produces reasonable DEP force without overheating and consequently damaging the NW during DEP process.

Finally, the DEP force is maximized for a ratio between the electrodes gap and the NW length of around 0.8, since the electric field gradient and strength effects are largest for this ratio.[18] For a smaller gap, the DEP force decreases because, despite that the electric field applied at the gap center remains constant, it is reduced around the entire NW length. On the other hand, for a larger gap, the DEP force still decreases, simply because the electric field around the NW is less intense.[18] In this work, for NiNW length of $(4 \pm 1)$ $\mu$m, we used a gap length of $(2.5 \pm 0.3)$ $\mu$m, yielding a ratio of $(0.6 \pm 0.2)$, which is near the maximum DEP force condition.

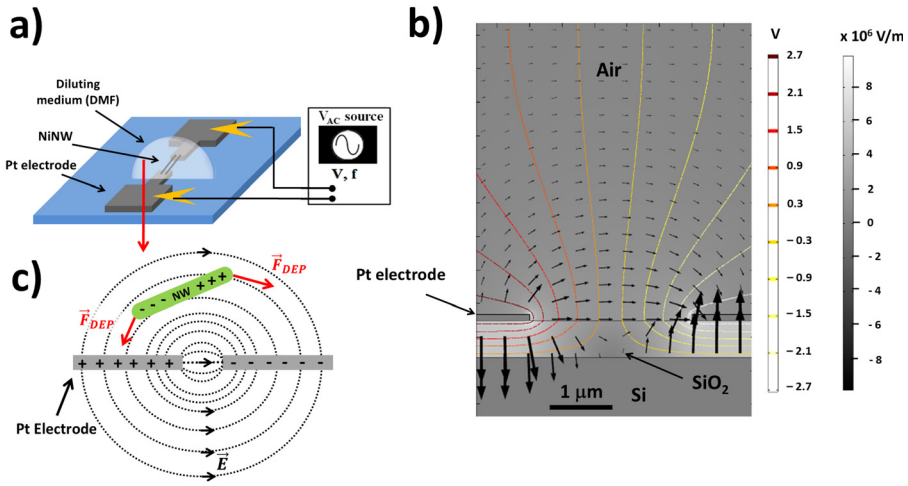


FIG. 1. (Color online) (a) Schematic of the DEP setup, (b) transversal view of total electric field and potential over the gap region of the electrodes structure, and (c) DEP mechanism, in which the electric field induces attraction forces on the nanowire toward the electrodes.

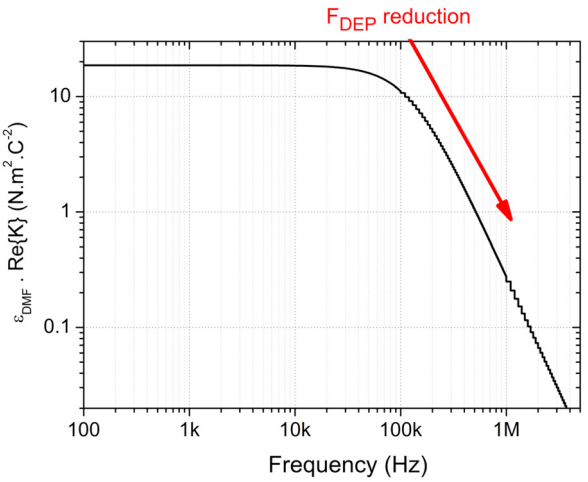


FIG. 2. (Color online) Real part of complex polarization factor (proportional to $F_{DEP}$) as function of frequency for DEP experiment of NiNW diluted in DMF, indicating a reduction of DEP force intensity over higher frequencies.

## III. EXPERIMENTAL DETAILS

Pt electrodes were defined on a $SiO_2$/Si structure. First, a 300 nm-thick $SiO_2$ layer was grown on an $n^+$-type Si (100) wafer (electrical resistivity of 1–10 Ω cm) by wet thermal oxidation in a conventional furnace, in order to act as a dielectric layer [Fig. 3(a)]. Then, photolithography was performed to define the electrodes region. Eighty nanometer-thick Pt layer was sputtered by a physical vapor deposition system, and lift-off process was carried out to define electrodes [Fig. 3(b)]. Three different electrodes geometries were fabricated to evaluate the effect of electrode shape on DEP force, further denominated #1 (rectangular extremities), #2 (circular extremities), and #3 (narrow extremities) (Fig. 4). The total electric field distribution over the gap area was simulated using COMSOL MULTIPHYSICS simulation tool.

NiNWs of $4 \pm 1$ $\mu$m-long and $35 \pm 5$ nm diameter were fabricated via pulsed electrodeposition into anodized alumina membrane.[19] They were released from the membrane by chemical etching with a 1 M NaOH solution at 27 °C under agitation. NiNW were then cleaned with deionized water (18 MΩ cm) and dispersed in DMF, in order to avoid NW clusters formation.

The NiNW deposition was performed by DEP, conducted with a HP 8116A pulse/function generator configured with 3 $V_{PP}$ and null offset [Fig. 3(c)]. The sinusoidal signal was generated for a frequency range between 50 kHz and 1 MHz. Before DEP process, the solution (concentration of $10^8$ NiNW/ml) was sonicated for 120 s, in order to uniformly disperse the NiNW into the DMF. For each pair of electrodes, the DEP field was applied during 60 s on a solution volume of 1 $\mu$l. The DMF excess was rinsed with deionized water (18 MΩ cm) before being dried with $N_2$. For each set of DEP parameters, the experiment was repeated several times to ensure statistical reliability (Table I).

Finally, a 10 nm-thick cap layer of Pt was deposited on the NiNW extremities to reduce the contact resistance with the electrodes [Fig. 3(d)], using a $Ga^+$ focused ion beam (GaFIB)/scanning electron microscope (SEM) with a gas injection system (GIS) tool.[20] This dual beam system may be used for micro- and nanofabrication in prototype nanomachining applications[21–23] and allows high resolution etching in nanoscale design without requiring lithography.[24]

The GIS is an available feature with the GaFIB/SEM dual beam system that allows the deposition, using ion or electron beams, of metallic materials, such as Pt.[20,25,26] The precursor gases are introduced very near the sample by the GIS and adsorbed on the substrate surface (Fig. 5). Secondary electrons, with energy in the range of 2–80 eV, are produced in the scanned region of the substrate by interaction with ion or electron beam, which crack precursor molecules over the defined area.[21,25] Volatile components of the process then leave the surface and are pumped away by the vacuum system. The precursors gas of Pt is a platinum-based organometallic compound $[(CH_3)_3PtCpCH_3]$.[21,25,26]

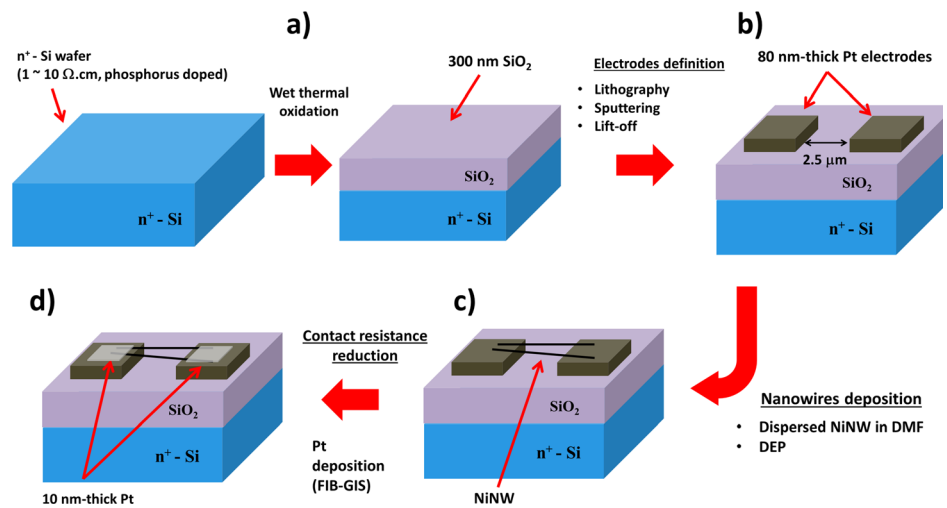


FIG. 3. (Color online) Schematics of experimental procedures: (a) dielectric layer formation on top of $n^+$-Si wafer by thermal oxidation; (b) electrodes definition by photolithography and lift-off; (c) NiNW deposition on electrodes by DEP experiment; and (d) contact resistance reduction after the deposition of Pt layer by GIS-FIB.

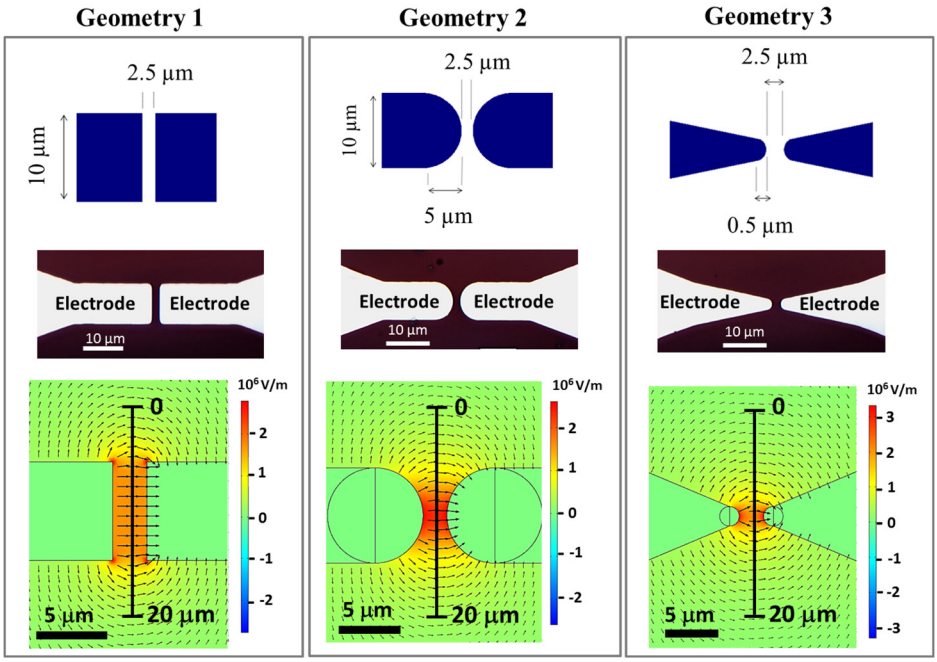


FIG. 4. (Color online) Schematics (top), optical microscopy (center), and total electric field simulations (below) of the three geometries tested for the Pt electrodes. The 20 $\mu$m line was taken for evaluation of the electric field profile for each geometry, as presented in Fig. 8.

The ion beam source used in this work was gallium ions ($Ga^+$) from a FEI Nova 200 Nanolab GaFIB/SEM dual beam system with energy of 30 keV, current of 10 pA and tilt angle of 0° (Fig. 5). Under these conditions, the milling process of NiNW and electrodes was significantly reduced. It is well known that ion beam induced deposition and milling processes damage the incident beam region by sputtering the surface and implanting ions.[23,27–29] The $Ga^+$ ion bombardment can cause an amorphous layer formation, as atoms are ejected by collisions and create vacancies, thus reducing the material conductivity.[23,27] Therefore, GaFIB process can modify the sample electrical and mechanical properties near the incidence region.[26–29] Simulations of the $Ga^+$ ions influence on the NiNW was obtained with TRIM software, a Monte Carlo computer program that calculates the interactions of energetic ions with targets.[30] With this tool, one can evaluate the stopping power and range of ions into matter, using a classical mechanical treatment of ion–atom collisions. This will be discussed in Sec. IV B.

TABLE I. Numbers of measurements taken for DEP efficiency investigation as function of applied field frequency and electrode geometry.

| | Geometry | | | |
|---|---|---|---|---|
| Frequency (kHz) | #1 | #2 | #3 | Total |
| 10 | 20 | 10 | 10 | 40 |
| 100 | 90 | 35 | 35 | 160 |
| 200 | 50 | 15 | 15 | 80 |
| 600 | 50 | 15 | 15 | 80 |
| 1000 | 50 | 15 | 15 | 80 |
| Total | 260 | 90 | 90 | 440 |

## IV. RESULTS AND DISCUSSION

### A. DEP efficiency

Visual inspection of the gap region by SEM was used to evaluate the DEP efficiency for the three electrode geometries and the frequency range used (Fig. 6). An experiment where at least one NiNW was deposited—and made electrical contact with a pair of electrodes—was considered as success. For each geometry and frequency, we normalized the number of successes by the total number of experiments (Table I). Thus, it was possible to evaluate the efficiency percentage of NiNW deposition [Fig. 7(a)] and the average number of deposited NiNW for the successful cases [Fig. 7(b)], as a function of the DEP frequency and electrode geometry.

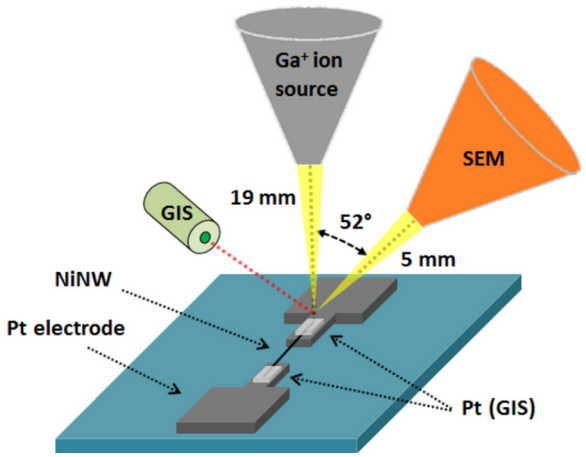


FIG. 5. (Color online) Schematic overview of GaFIB/SEM dual beam system, with the GIS feature.

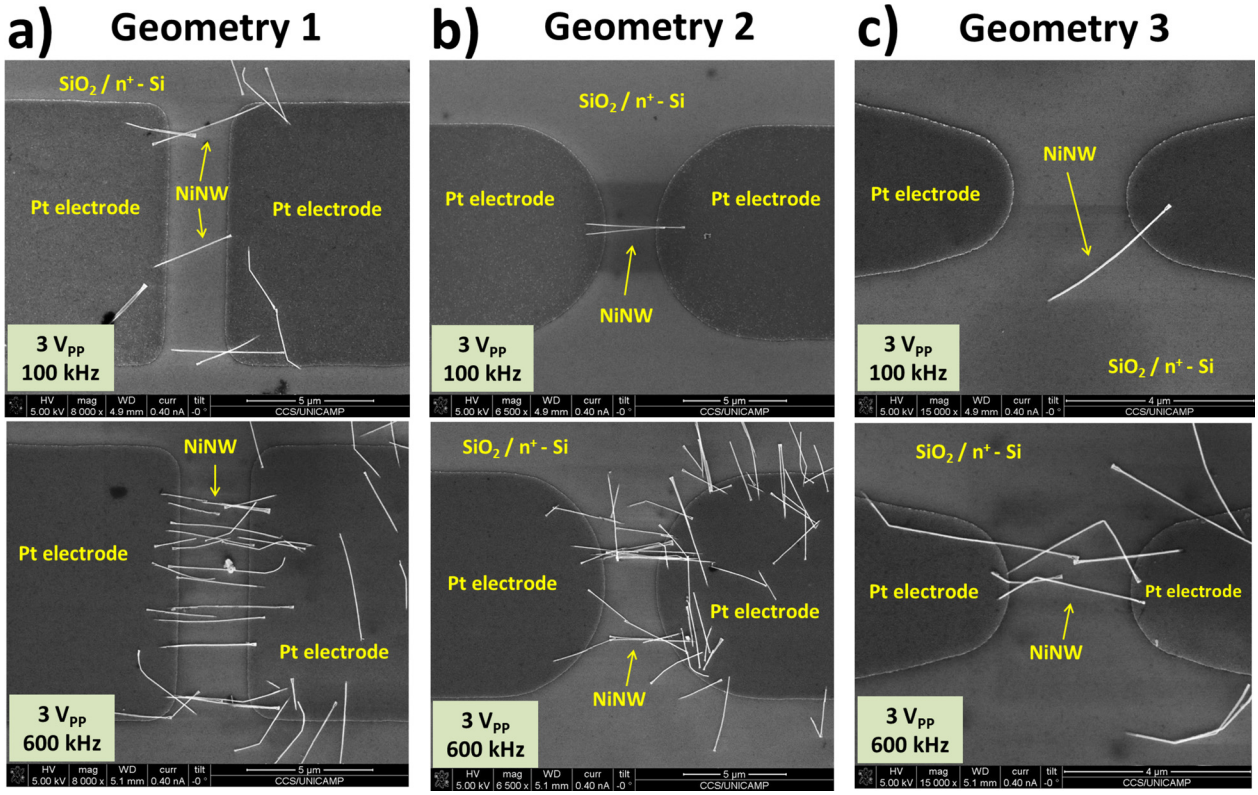


FIG. 6. (Color online) Typical SEM analysis of NiNW deposited on Pt electrodes for (a) geometry #1, (b) geometry #2, and (c) geometry #3, after DEP experiment ($V_{PP} = 3$ V, frequency = 100 kHz (upper row), and 600 kHz (lower row).

First, as expected from Eq. (4) and fluid dynamics effects predictions, the DEP efficiency at 10 kHz and 1 MHz was almost null, obtaining success only for geometry 1 (8% and 16%, respectively). The maximum efficiency obtained for geometry 1 was 85% at 100 kHz, while an efficiency of 60% was still reached at 600 kHz. On the other hand, the DEP process was less efficient for geometries 2 and 3, both with maximum value of 50% obtained for 600 kHz. This discrepancy may be assigned to electric field homogeneity over the electrodes gap, which is larger for geometry 1 than for geometries 2 and 3. The electrode areas are smaller in geometry 2 and 3 cases, which could create inhomogeneities and thus reduce the trapping region in the gap region. For geometry 1, the larger electrode area increases the probability of success and captures more NiNW during DEP process. Figure 8 presents the simulated total electric field intensity along a 20 $\mu$m transversal cross-section in the gap region, indicated in Fig. 4. We assume that the product between the peak height, $h$, and its full-width half-maximum, $\sigma$, is related to the deposition efficiency. The decreasing product value for geometry #1 to #3 is in agreement with the obtained efficiency results.

Typically, several NiNWs were simultaneously deposited during the successful experiments, with an average number ranging from 1.0 to 8.7. Interestingly, for each geometry investigated, the higher number of deposited NiNW was not reached for the frequency yielding the highest efficiency. For geometry 1, only 3.4 NiNWs were deposited at 100 kHz

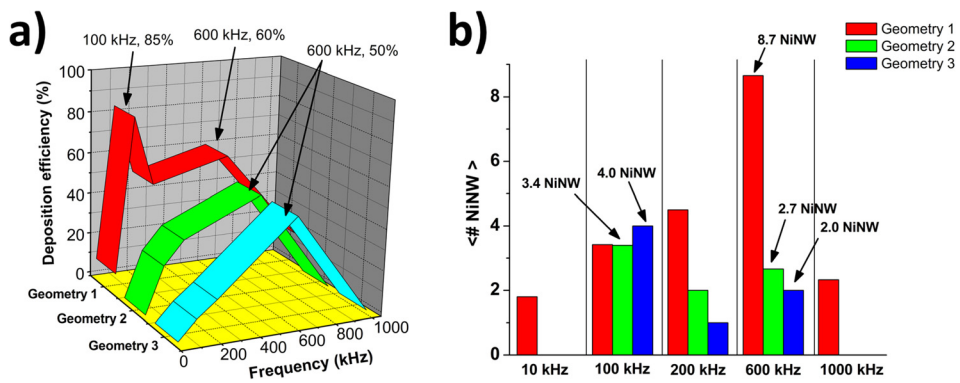


FIG. 7. (Color online) Charts of (a) deposition efficiency and (b) average number of deposited NiNW, obtained for DEP experiment as a function of electric field frequency, for the three electrodes geometries.

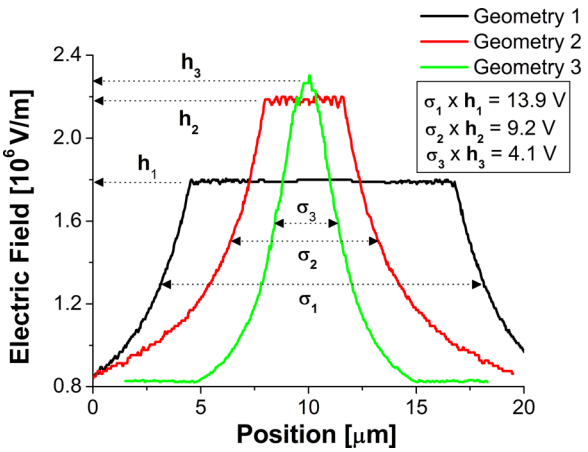


FIG. 8. (Color online) Total simulated electric field amplitude profile for the 20 $\mu$m transversal line showed in Fig. 4 for the three geometries, indicating the trapping efficiency to be related to the product between the peak height and its full-width half-maximum.

(85% of efficiency), while a peak of 8.7 ones was attained at 600 kHz (60% of efficiency). The situation is similar for geometries 2 and 3, but inverting the frequencies for which the efficiency and number of deposited NiNWs are maximum (Fig. 7). The large number of deposited NiNWs even for low efficiency frequency may be attributed to the distortion of the electric field in the electrodes gap created by the first deposited NiNW, favoring the DEP force on the remaining NiNW in the DMF solution.

Globally, geometry 1 is the most efficient for DEP of NiNW, as one can obtain efficiency up to 85% (for 3 $V_{PP}$ and 100 kHz). However, our aim when using DEP process was the evaluation of NiNW transport properties and fabrication of devices with a few NW. Thus, a reasonable result is obtained when only a few NiNW are present between electrodes. Therefore, geometries 2 and 3 reach ideal average values of NiNW (2.7 and 2.0, respectively, for 600 kHz), still with 50% of efficiency.

### B. Reduction of contact resistance using GaFIB

As shown, DEP is an adequate tool to insert NW between electrodes for electrical transport measurements. However, when the nanowire touches the electrodes, a large contact resistance is usually present, leading to a Schottky-like contact (nonlinear). After depositing a 10 nm-thick cap layer of Pt on the NiNW extremities to reduce the contact resistance, the resulting behavior is ohmic (linear).[20] Figure 9(a) presents the parallel-equivalent resistance as a function of the number of deposited NW, both in logarithmic scale, before and after Pt deposition. The linear fit slopes ($-1.2 \pm 0.2$ for as-deposited NiNW) and ($-1.0 \pm 0.1$ after Pt deposition) are in agreement with the ideal case ($-1$), which confirms the parallel-equivalent resistance law for the NiNW. In addition, the offset between the linear fits indicates the resistance reduction by the Pt deposition method using GaFIB/SEM and GIS.

In the current study, we obtained current ($I$) versus voltage ($V$) curves by applying current—without exceeding 6 $\mu$A to avoid NiNW damage due to heat dissipation—while measuring voltage with a four-wire setup. We observed a transformation from a nonlinear behavior for as-deposited system to a linear one, after Pt layer deposition, as well as a resistance reduction [Fig. 9(b)]. From the obtained NiNW resistance (6 k$\Omega$) after subtracting the electrodes resistance contribution (120 $\Omega$), we obtained a resistivity value for NiNW ($\rho_{NiNW} = 1.3 \times 10^{-5}\,\Omega\,cm$) that is consistent with those of similar dimensions.[31]

In order to evaluate the effects of $Ga^+$ implantation on NiNW, simulations of their interactions were carried out under similar conditions as the experimental ones (30 keV and tilt angle of 0°) using TRIM software. Figures 10(a) and 10(b) show, respectively, the depth profiles of ion range and damage (creation of atomic vacancies in the target material) of gallium ions in the NiNW/Pt electrodes structure at the region of ionic bombardment for Pt deposition by GaFIB. We observed a range of $10 \pm 5$ nm for the $Ga^+$ ions penetration into the NW, yielding to an amorphization depth of around 25 nm in the region of Pt deposition. This process therefore leaves a thickness of at least 10 nm of polycrystalline NiNW not reached by $Ga^+$ ions, i.e., the damage created is not over the entire NW diameter. The resistance of the resulting structure increases around one order of magnitude to this effect. Nevertheless, the Pt deposition was limited to the NW very extremities to prevent increase of their resistance by Ga amorphization.

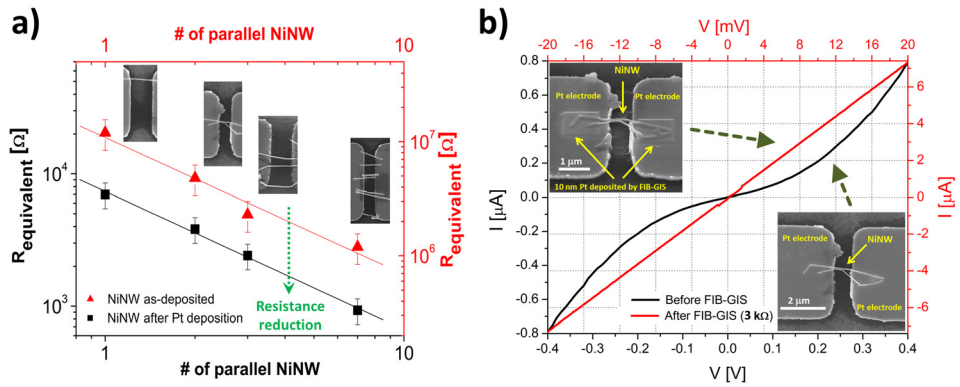


FIG. 9. (Color online) (a) Equivalent parallel resistance vs number of parallel deposited NiNW before and after Pt deposition. (b) $I \times V$ curves for NiNW before (non-linear, left and down axes) and after (linear, right and up axes) 10 nm-thick Pt layer deposition by GIS tool of GaFIB.

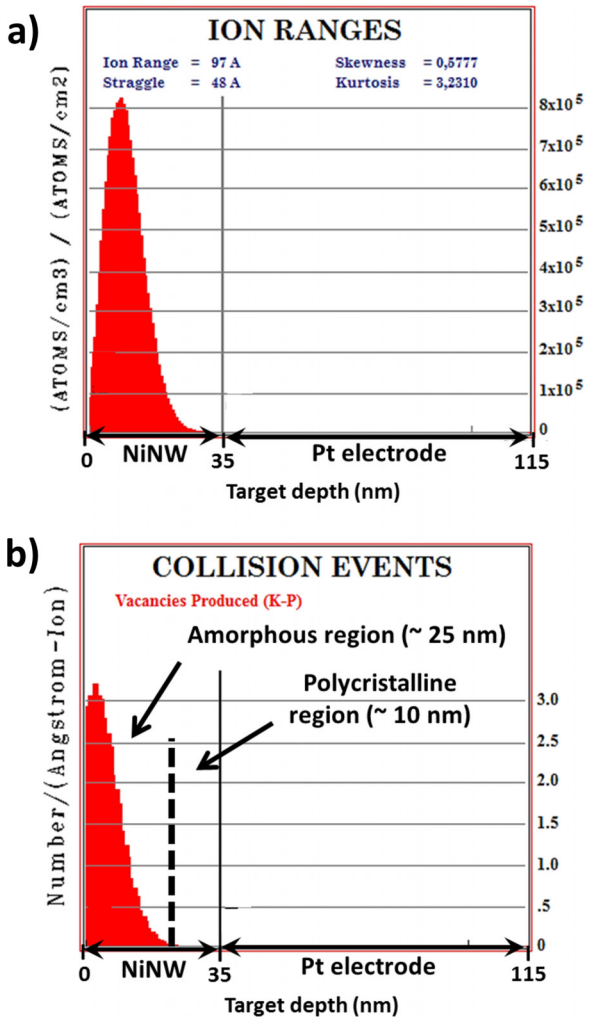


FIG. 10. (Color online) Depth profiles of (a) $Ga^+$ ions implantation range and (b) damage (vacancies produced) after deposition of 10 nm-thick Pt cap layer by GaFIB.

## V. SUMMARY AND CONCLUSIONS

This work presented DEP manipulation of NiNW over Pt electrodes defined by photolithography and lift-off. The deposition efficiency and average number of NiNW were evaluated as a function of the electrode geometry and DEP frequency. The maximum deposition efficiencies for geometry 1 were 85% and 60% for 100 and 600 kHz, respectively, for averages of 3.4 and 8.7 deposited NiNW. On the other hand, the efficiency was maximized at 600 kHz for geometries 2 and 3, with value of 50% and averages of 2.7 and 2.0 NiNW, respectively. This behavior can be attributed to electric field inhomogeneities and lower trapping area over the gap present between electrodes geometries 2 and 3. For geometry 1, since it presents a larger electrode area, it captures more NiNW during DEP process and increases the probability of success, even with electric field intensity slightly lower than geometries 2 and 3.

Adequate individual NiNW electrical measurements are allowed by the successful contact resistance reduction through deposition of 10 nm-thick Pt cap layer on the NW extremities by GIS-GaFIB. Simulated results showed the NiNW resistance increased due to $Ga^+$ ion damage caused does not prohibit the process adequacy.

Moreover, the studied NiNWs are a promising feature to be used as sensors devices, since they can be manipulated with high efficiency to make contact with electrodes and their electrical, thermal, and/or optical output signals (in response to the environment stimulus) can be further processed.[32] In addition, NiNWs present ferromagnetic properties, which allow their low current levels to be controlled through magnetic fields. Thus, they can be thought as a promising alternative to the traditional Si-based MOSFET devices.

## ACKNOWLEDGMENTS

The authors would like to thank CCS/UNICAMP and LMBT/IFGW/UNICAMP staff for device processing and characterization. The work was supported by the Brazilian funding agencies Fundação de Amparo à Pesquisa do Estado de São Paulo (FAPESP), Conselho Nacional de Desenvolvimento Científico e Tecnológico (CNPq) and Coordenação de Aperfeiçoamento de Pessoal de Nível Superior (CAPES).

[1]J. Wu, B. Yin, F. Wu, Y. Myung, and P. Banerjee, Appl. Phys. Lett. **105**, 183506 (2014).
[2]M. Li, W. H. Li, J. Zhang, G. Alici, and W. Wen, J. Phys. D: Appl. Phys. **47**, 063001 (2014).
[3]K. W. Seo, J. H. Lee, N. G. Cho, S. J. Kang, H. K. Kim, S. I. Na, H. W. Koo, and T. W. Kim, J. Vac. Sci. Technol. A **32**, 061201 (2014).
[4]M. N. Ou, T. J. Yang, S. R. Harutyunyan, Y. Y. Chen, C. D. Chen, and S. J. Lai, Appl. Phys. Lett. **92**, 063101 (2008).
[5]J. J. Boote and S. D. Evans, Nanotechnology **16**, 1500 (2005).
[6]A. W. Maijenburg, M. G. Maas, E. J. B. Rodijk, W. Ahmed, E. S. Kooij, E. T. Carlen, D. H. A. Blank, and J. E. ten Elshof, J. Colloid Interface Sci. **355**, 486 (2011).
[7]B. C. Gierhart, D. G. Howitt, S. J. Chen, R. L. Smith, and S. D. Collins, Langmuir **23**, 12450 (2007).
[8]C. Xie, B. Chen, C. O. Ng, X. Zhou, and J. Wu, Eur. J. Mech. B **49**, 208 (2015).
[9]S. Kang, Comput. Fluids **105**, 231 (2014).
[10]M. I. Schukfeh, K. Storm, A. Hansen, C. Thelander, P. Hinze, A. Beyer, T. Weinmann, L. Samuelson, and M. Tornow, Nanotechnology **25**, 465306 (2014).
[11]F. S. Hamdi, O. Français, E. D. Gergam, and B. L. Pioufle, Bioelectrochemistry **100**, 27 (2014).
[12]E. M. Freer, O. Grachev, X. Duan, S. Martin, and D. P. Stumbo, Nat. Nanotechnol. **5**, 525 (2010).
[13]H. A. Pohl, *Dielectrophoresis: The Behavior of Neutral Matter in Non-Uniform Electric Fields* (Cambridge University, Cambridge, 1978).
[14]H. A. Pohl, J. Appl. Phys. **22**, 869 (1951).
[15]S. Raychaudhuri, S. A. Dayeh, D. Wang, and E. T. Yu, Nano Lett. **9**, 2260 (2009).
[16]W. Xue and P. Li, in *Dielectrophoretic Deposition and Alignment of Carbon Nanotubes, Carbon Nanotubes—Synthesis, Characterization, Applications*, edited by S. Yellampalli (InTech, Rijeka, Croatia, 2011).
[17]M. Dimaki and P. Boggild, Nanotechnology **15**, 1095 (2004).
[18]Y. Liu, J. H. Chung, W. K. Liu, and R. S. Ruoff, J. Phys. Chem. B **110**, 14098 (2006).
[19]D. C. Leitao, C. T. Sousa, J. Ventura, J. S. Amaral, F. Carpinteiro, K. R. Pirota, M. Vazquez, J. B. Sousa, and J. P. Araujo, J. Non-Cryst. Solids **354**, 5241 (2008).
[20]L. P. B. Lima, M. V. P. dos Santos, F. H. Cioldin, J. A. Diniz, I. Doi, and J. Godoy Fo, ECS Trans. **49**, 367 (2012).
[21]M. V. Puydinger dos Santos, L. P. B. Lima, J. A. Diniz, and J. G. Filho, J. Vac. Sci. Technol. B **31**, 06FA01 (2013).
[22]K. A. Unocic, M. J. Mills, and G. S. Daehn, J. Microsc. **240**, 227 (2010).

[23]S. E. Wu and C. P. Liu, Nanotechnology **16**, 2507 (2005).
[24]I. M. Ross, W. H. Ng, L. R. Wilson, I. J. Luxmoore, J. W. Cockburn, A. Krysa, A. G. Cullis, and J. S. Roberts, J. Phys.: Conf. Ser. **26**, 215 (2006).
[25]S. Waid, H. D. Wanzenboeck, M. Muehlberger, M. Gavagnin, and E. Bertagnolli, J. Vac. Sci. Technol. B **32**, 041602 (2014).
[26]I. Utke, P. Hoffmann, and J. Melngailis, J. Vac. Sci. Technol. B **26**, 1197 (2008).
[27]S. Rubanov and P. R. Munroe, J. Microsc. **214**, 213 (2004).
[28]F. Lenrik, M. Ek, D. Jacobsson, M. T. Borgström, and L. R. Wallenberg, Microsc. Microanal. **20**, 133 (2014).
[29]R. P. Chauhan and P. Rana, J. Radioanal. Nucl. Chem. **302**, 851 (2014).
[30]J. F. Ziegler, J. P. Biersack, and M. D. Ziegler, *SRIM: The Stopping and Range of Ions in Matter* (Chester, Maryland, 2008).
[31]S. Mani, T. Saif, and J. H. Han, IEEE Trans. Nanotechnol. **5**, 138 (2006).
[32]U. Yogeswaran and S. M. Chen, Sensors **8**, 290 (2008).